

Pairing in $SU(6) \times SU(2)$ one-dimensional fermionic clusters

M.C. Gordillo

*Departamento de Sistemas Físicos, Químicos y Naturales,
Universidad Pablo de Olavide. E-41013 Seville, Spain*

We present diffusion Monte Carlo (DMC) calculations on the behavior of a mixture of ^{173}Yb and ^{171}Yb fermionic isotopes in a one-dimensional environment. The interaction parameters between species were modeled by delta potentials, whose strengths were taken from their experimental scattering lengths and varied by changing the transversal confinement. This implies a repulsive interaction for the ^{173}Yb - ^{173}Yb pair, a strong attractive one for the ^{173}Yb - ^{171}Yb set and a weak attraction between ^{171}Yb - ^{171}Yb atoms. Those arrangements were described by a corrected geminal multiplied by the appropriate set of Jastrow functions. We found that, for the same number of strong attractive pairs, the width of the cluster decreases when the number of fermionic species increases, the narrower cluster being the one that includes a mixture of six ^{173}Yb species and two ^{171}Yb spin types.

I. INTRODUCTION

The majority of experiments on ultracold fermions deal with alkali atoms, such as ^6Li and ^{40}K [1]. Since we can find those fermions in two different spin states, all those systems have $SU(2)$ symmetry. However, the nuclear and electronic structures of alkali-earth metal atoms, like ^{87}Sr , allow them to populate up to ten spin states [2, 3]. A similar behavior is experimentally found in ^{173}Yb , with up to six different spin values [4–6]. Moreover, the ytterbium isotope family is quite complex, with seven components: two fermions and five bosons [7]. This allows a wide range of mixtures, such as the experimentally realized $SU(6) \times SU(2)$ (two kinds of fermions, ^{173}Yb with $SU(6)$ symmetry and ^{171}Yb with $SU(2)$ one) [8, 9], or the one including ^{173}Yb atoms and two different types of bosons (^{170}Yb or ^{174}Yb) [10]. Most of the experimental data for those systems deal with their behavior when loaded in optical lattices. In this work, however, we will study harmonically-confined (quasi) one-dimensional (1D) arrangements, similar to the ones considered experimentally in Ref. 4. The main difference will be that, instead of taking into account exclusively ^{173}Yb fermions interacting repulsively, we will consider 1D mixtures of fermions that not only repel but attract each other.

In consonance with all of the above, the modelization of $SU(N)$ arrangements is usually done only for atoms loaded in optical lattices, and by means of discrete Hamiltonians, specially the Hubbard model [2, 11–14]. However, some descriptions of 1D harmonically-confined continuous models are available in the literature [15–18], all of them considering only repulsive interspecies interactions. The continuous Hamiltonian that can be used to describe those systems is:

$$H = \sum_{i=1}^{N_p} \left[\frac{-\hbar^2}{2m} \nabla_i^2 + \frac{1}{2} m \omega^2 x_i^2 + V_{ext}(x_i) \right] + g_{1D}(\alpha, \beta) \sum_{\alpha=1}^N \sum_{\beta>\alpha}^N \sum_{i=1}^{N_\alpha} \sum_{j=1}^{N_\beta} \delta(x_i^\alpha - x_j^\beta). \quad (1)$$

Here, N is the number of spin species, and N_p the total

number of particles. Even though we considered mixtures of ^{173}Yb and ^{171}Yb , we judged their masses to be similar enough to assign them the same value, m . $\sigma = \sqrt{\hbar/m\omega}$ is the so-called oscillator length, in this case in the longitudinal direction, i.e., the one parallel to the 1D coordinate the atoms are allowed to move along. As it is customary, this will be our unit of length, and was calculated from the experimental ω value given in Ref. 4 ($\omega = 2\pi \times 80$ Hz). The interaction strength between particles was modeled by delta functions depending on the pair of species, (α, β) , considered via their respective g_{1D} parameters, with $g_{1D}(\alpha, \beta) = -2\hbar^2/ma_{1D}(\alpha, \beta)$. $g_{1D}(\alpha, \beta)$ is positive for repulsive interactions, and negative for attractive ones. Here, $a_{1D}(\alpha, \beta)$ is the one-dimensional scattering length of the pair, that can be obtained from its three-dimensional experimental counterpart, $a_{3D}(\alpha, \beta)$, using [19]:

$$a_{1D}(\alpha, \beta) = -\frac{\sigma_\perp^2}{2a_{3D}(\alpha, \beta)} \left(1 - A \frac{a_{3D}(\alpha, \beta)}{\sigma_\perp} \right), \quad (2)$$

with $A=1.0326$. σ_\perp is another oscillator length, in this case in the perpendicular direction to the one the Yb atoms are allowed to move. This means that, for the same values of a_{3D} , we can have different values of a_{1D} by changing the value of ω_\perp , that experimentally is in the range of kHz [4, 10]. The $a_{3D}(\alpha, \beta)$ values are 10.55 nm (^{173}Yb - ^{173}Yb), -0.15 nm (^{171}Yb - ^{171}Yb) and -30.6 nm (^{171}Yb - ^{173}Yb) [7], with the minus signs standing for attractive interactions. The g_{1D} values for the different pairs, calculated using Eq. (2), are shown in Fig. 1 as a function of ω_\perp . One can easily see that while g_{1D} for the ^{171}Yb - ^{171}Yb pair is very weakly attractive for the entire range of confinements considered, the ^{171}Yb - ^{173}Yb parameter is always strongly attractive, while the one for the ^{173}Yb - ^{173}Yb pair is repulsive.

II. METHOD

We solved the Schrödinger equation derived from the Hamiltonian in Eq. (1) using the Fixed-node diffusion

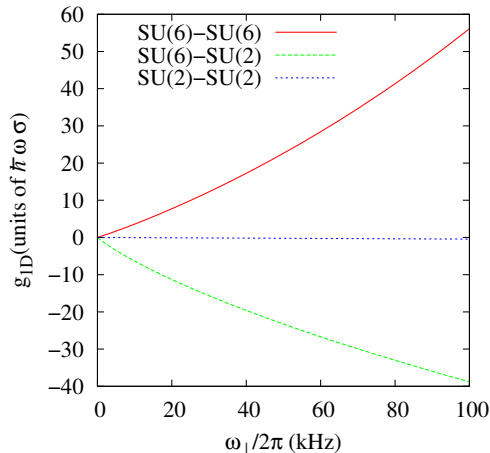


FIG. 1. Values of the g_{1D} parameters for the different pairs of Yb isotopes as a function of confinement, represented by the harmonic oscillation perpendicular frequency, ω_{\perp} .

Monte Carlo (FN-DMC) method. This technique allows us to obtain stochastically the exact ground state energy of a system of fermions when the positions of the nodes of the exact many-body wavefunction that describes them are known [20]. Fortunately, this condition is fulfilled in strictly 1D systems, since we can have nodal points only when two particles of the same species are at the same position [21]. For the DMC algorithm to work, we need an initial approximation of the real many-body function of the system. This is called the *trial function* and for an arrangement of repulsively interacting ^{173}Yb particles belonging to different spin states can be written as [15–17]:

$$\Phi(x_1, \dots, x_{N_p}) = \prod_{\alpha=1}^N D^{\alpha} \prod_i^{N_{\alpha}} \prod_j^{N_{\beta}} \psi(x_i^{\alpha} - x_j^{\beta}), \quad (3)$$

where the Slater determinant D^{α} , for atoms belonging to the α spin species, contains the lowest N_{α} eigenvectors corresponding to a non-interacting version of the Hamiltonian in Eq. (1). In this particular case, this means the one-body harmonic oscillator functions that can be found in any textbook. It is well known that when this happens, D^{α} can be given as a product of Gaussian functions

and a Van der Monde determinant [22]:

$$D^{\alpha} = C \left(\prod_i \exp[-x_i^2/2] \right) \left(\prod_{1 < j < l < N_{\alpha}} (x_l - x_j) \right), \quad (4)$$

with C the proper normalization constant. $\psi(x_i^{\alpha} - x_j^{\beta})$ is the so-called Jastrow function, that takes into account the correlations between particles not belonging to the same spin species. In 1D systems, that Jastrow function is usually taken as the solution of the homogeneous Hamiltonian in Eq. (1) for two particles [23, 24], and it is different for repulsive and attractive δ interactions.

In the first case, we took the short-range solution given in Ref. 24, used in previous works [17, 18, 24–28]:

$$\psi(x_i^{\alpha} - x_j^{\beta}) = \begin{cases} \cos(k[|x_i^{\alpha} - x_j^{\beta}| - R_m]) & |x_i^{\alpha} - x_j^{\beta}| < R_m \\ 1 & |x_i^{\alpha} - x_j^{\beta}| \geq R_m \end{cases} \quad (5)$$

Here, R_m is the only variationally optimized parameter, found to be 10σ for all the system considered in this work. Once that parameter was fixed, k could be obtained by numerically solving the transcendental equation:

$$ka_{1D}(\alpha, \beta) \tan(kR_m) = 1, \quad (6)$$

for each value of $a_{1D}(\alpha, \beta)$ [24].

On the other hand, the interaction could be attractive, and then the homogeneous solution of Hamiltonian of Eq. (1) for two particles [30], used as a Jastrow, is [23, 24]:

$$\phi(|x_i^{\alpha} - x_j^{\beta}|) = \exp \left[-\frac{|g_{1D}(\alpha, \beta)|}{2} |x_i^{\alpha} - x_j^{\beta}| \right]. \quad (7)$$

This function does not depend on any adjustable parameters.

For a system that includes exclusively repulsive interactions, it is very easy to see that Eq. (3) is equivalent to:

$$\Phi(x_1, \dots, x_{N_p}) = D \prod_i^{N_{\alpha}} \prod_j^{N_{\beta}} \frac{\psi(x_i^{\alpha} - x_j^{\beta})}{(x_i^{\alpha} - x_j^{\beta})}, \quad (8)$$

with D a Slater determinant including *all* N_p one-body functions. On the other hand, it is well known that a trial function of the form given by Eq. 3 does not work properly when the particles making up the system attract each other. In the case we have only two kind of fermions, the trial function has the form of a geminal [29, 31, 32]:

$$\Phi(x_1, \dots, x_{N_p}) = \mathcal{A}[\phi(r_{11'})\phi(r_{22'}) \cdots \phi(r_{N_p/2, N_p'/2})] \quad (9)$$

where \mathcal{A} is an antisymmetric operator, and $\phi(r_{ij'})$ a pair function depending on the distance between two particles with different spins, $r_{ij'} = |x_i - x_j|$, that in our case is the same that the one given by Eq. (7).

In this work, instead of having only two different sets of particles, we consider mixtures of ^{173}Yb and ^{171}Yb

atoms with the particularity that not all the particles in the N_{173} subset are indistinguishable, but belong to up to 6 different spin types. The same can be said of the ^{171}Yb ensemble, made up of up to two different kinds of particles that attract each other. With that in mind, a naive form for the trial function could be:

$$\Phi(x_1, \dots, x_{N_p}) = \prod_i \exp[-x_i^2/2] \prod_i \prod_j \psi(x_i^\alpha - x_j^\beta) \times \mathcal{A}[\phi(r_{11'})\phi(r_{22'}) \dots \phi(r_{N_{173}, N_{171}})] \quad (10)$$

in which α and β stand for different species *within* the ^{173}Yb and ^{171}Yb subsets. The strongly attractive (^{173}Yb - ^{171}Yb) cross interaction is taken into account by using the geminal, in which every element of the determinant depends on the distance, r , between a ^{173}Yb atom and a ^{171}Yb one. The trial function in Eq. (10) is antisymmetric only with respect to the interchange of particles belonging to species with the same spin. The introduction of the Jastrow terms forbids that antisymmetric character when the atoms are distinguishable. However, it can only provide an upper bound to the energy of the real system, since its geminal part has nodes when $(x_i^\alpha - x_j^\beta) = 0$, i.e., when atoms belonging to the same set (^{173}Yb or ^{171}Yb) but with different spins are on top of each other, which it is not necessarily realistic.

To correct that, we have to look at the geminal structure. If we consider two consecutive rows describing the interaction of two distinguishable atoms at coordinates x_i and x_j in the ^{173}Yb subset with all the ^{171}Yb particles (at coordinates $x_{1'}, x_{2'}, \dots, x_{N_{171}'}$), we have:

$$\begin{vmatrix} \exp(-|g_{1D}|r_{i1'}/2) & \dots & \exp(-|g_{1D}|r_{i, N_{171}'}/2) \\ \exp(-|g_{1D}|r_{j1'}/2) & \dots & \exp(-|g_{1D}|r_{j, N_{171}'}/2) \end{vmatrix}$$

when $x_i \rightarrow x_j$, we can write

$$\begin{aligned} \phi(r_{ik'}) &= \exp(-|g_{1D}||x_i - x_{k'}/2) \\ &= \exp(-|g_{1D}||x_j + \Delta - x_{k'}/2) \end{aligned} \quad (11)$$

with $\Delta = x_i - x_j \rightarrow 0$. Expanding to the first order in Δ , we have:

$$\phi(r_{ik'}) = \phi(r_{jk'}) - g_{1D} \frac{\exp(-|g_{1D}|r_{jk'}/2)(x_j - x_{k'})\Delta}{2r_{jk'}} \quad (12)$$

Bearing in mind the properties of the determinants, we can see that the origin of the spurious node at $x_i - x_j \rightarrow 0$ is the dependence of all the elements of the geminal row that includes the i atom, on Δ . This can be corrected by dividing the trial function by, in this case, $x_i - x_j$. We can repeat this procedure for any pair of distinguishable atoms in the ^{173}Yb and ^{171}Yb ensembles. This means using a trial function similar to that of Eq. (8), but changing the Slater determinant by a geminal, i.e.:

$$\Phi(x_1, \dots, x_{N_p}) = \mathcal{A}[\phi(r_{11'})\phi(r_{22'}) \dots \phi(r_{N_6, N_2})] \prod_i \exp[-x_i^2/2] \prod_i \prod_j \frac{\psi(x_i^\alpha - x_j^\beta)}{(x_i^\alpha - x_j^\beta)}, \quad (13)$$

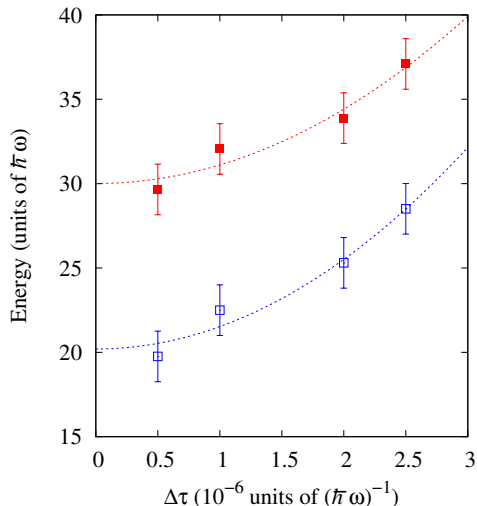


FIG. 2. Total energy of a system with 18 ^{173}Yb atoms with SU(6) symmetry and a single ^{171}Yb impurity for two different perpendicular confinements and as a function of the DMC time step, $\Delta\tau$. Upper curve, $\omega_{\perp} = 2\pi \times 20$ kHz; lower curve, $\omega_{\perp} = 2\pi \times 25$ kHz. The values of the energies and error bars are the result of averaging three independent configurations for each value of $\Delta\tau$. All data correspond to 1000 walkers. Fits corresponds to least-squares fits to the form $e(\Delta\tau) = a(\Delta\tau)^2 + e_0$.

this being the trial function used in the DMC calculations reported in this work. If instead of a system with the same total number of ^{173}Yb and ^{171}Yb atoms (that we term a *balanced* system), we have an *imbalanced* one, we followed the prescription of Ref. 29, and changed the geminal in Eq. (13) by a determinant including as many rows (or columns) of pairing functions as the number of particles in the minority component, and with the remaining rows filled by standard one-particle harmonic oscillator functions.

To avoid biases in the energies obtained by DMC, extra care was used to avoid spurious correlations. In particular, any energy value given is the average of three independent DMC calculations, with an error bar corresponding to those three values, and not to the statistical fluctuations typical of a DMC calculation. To decorrelate further, each of those three values were averages made considering the energies obtained every 200 Monte Carlo steps. This means that in a typical 10^6 step simulation (after thermalization), only 5000 values were used to calculate the energy. The other possible sources of bias were the DMC time step and the number of walkers [33]. To avoid the first, we extrapolated the values of the energy to the limit $\Delta\tau \rightarrow 0$, using the quadratic dependence corresponding to the propagator used [34]. Two examples of this procedure are given in Fig. 2. Those correspond to $30.0 \pm 0.7 \hbar\omega$ (upper curve), and $20.2 \pm 0.7 \hbar\omega$, very close to the values corresponding to the small-

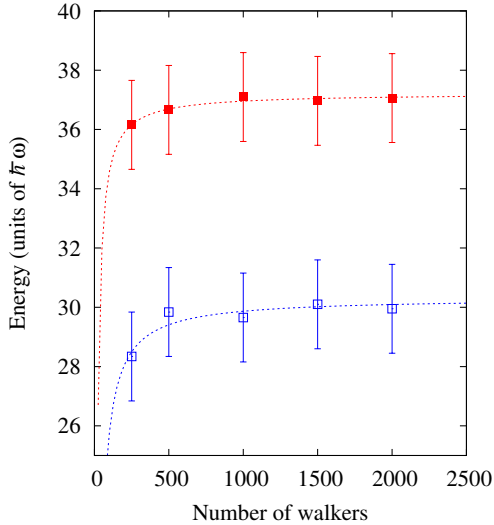


FIG. 3. Same as in the previous figure, but as a function of the number of walkers, N_w , for a perpendicular confinement equal to $\omega_{\perp} = 2\pi \times 20$ kHz. Upper curve, $\Delta\tau = 2.5 \cdot 10^{-6} (\hbar\omega)^{-1}$; lower curve, $\Delta\tau = 0.5 \cdot 10^{-6} (\hbar\omega)^{-1}$. The lines correspond to least-squares fits to the form $e(N_w) = a/N_w + e_{\infty}$.

est time step used, $0.5 \cdot 10^{-6} (\hbar\omega)^{-1}$ (29.7 ± 1.5 and $19.8 \pm 1.5 \hbar\omega$, respectively). The small differences between the results corresponding to $\Delta\tau = 0.5 \cdot 10^{-6} (\hbar\omega)^{-1}$ and the extrapolations to $\Delta\tau \rightarrow 0$, in any case larger than the error bars (in the range 1-2 $\hbar\omega$ for all energy values), make safe the use of the latter instead of the former as estimations of the energy.

On the other hand, once the appropriate de-correlation have been done following the procedure outlined above, it can be shown that the influence of the number of walkers, N_w , in the results is basically negligible. A couple of examples of this is given in Fig. 3. The energy values obtained by extrapolating to the limit $N_w \rightarrow \infty$ is $e_{\infty} = 37.2 \pm 0.1 \hbar\omega$ for $\Delta\tau = 2.5 \cdot 10^{-6} (\hbar\omega)^{-1}$ (upper curve) in Fig. 3, and $e_{\infty} = 30.3 \pm 0.1 \hbar\omega$ for $\Delta\tau = 0.5 \cdot 10^{-6} (\hbar\omega)^{-1}$ (lower curve in the same figure). Both numbers are well within the error bars of the energies corresponding to $N_w = 1000$. This is in consonance with the results of Ref. 33 for a system of bosons. There, it is stated that, at least for clusters of the size of the ones considered in this work, there is not an appreciable energy bias due to this cause, and that at least part of the problem in larger clusters could be the correlation between walkers. For uncorrelated configurations, the energy should depend inversely on that number, that is exactly what we see in Fig. 3. For that reason, we used 1000 walkers for most of our calculations.

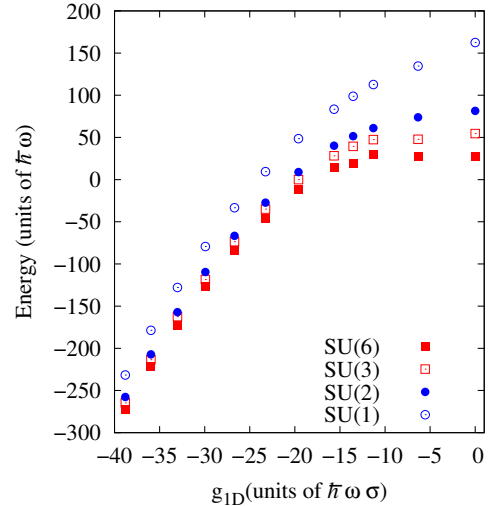


FIG. 4. Total energy of a system with 18 ^{173}Yb atoms and a single ^{171}Yb impurity as a function of the ^{173}Yb - ^{171}Yb interaction parameter. The ^{173}Yb atoms could have the same all the same spin (SU(1)), belong to two or three different spin sets (SU(2) and SU(3) respectively), or are distributed in six sets of three atoms each (SU(6)). The error bars are of the size of the symbols and are not shown for simplicity.

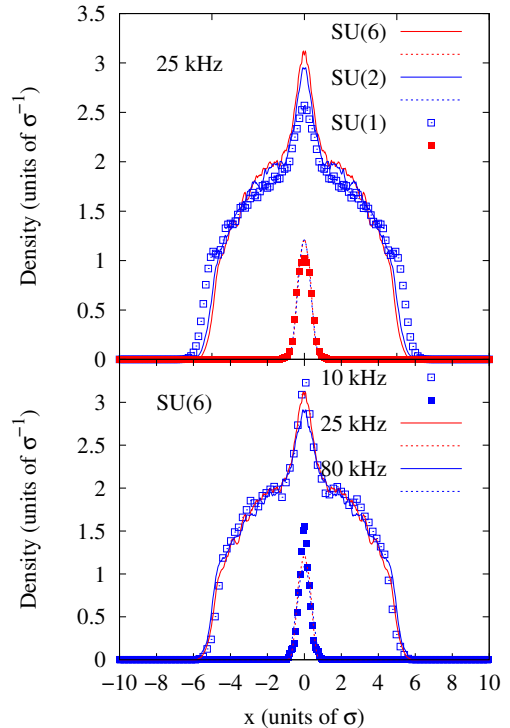


FIG. 5. Density profiles for the same systems as in the previous figure. Upper panel, a ^{171}Yb impurity embedded in different ^{173}Yb arrangements with the same perpendicular confinement ($\omega_{\perp} = 2\pi \times 25$ kHz). Lower panel, SU(6) + impurity profiles for different confining perpendicular frequencies.

III. RESULTS

Taking all of that in mind, we studied first the behavior of a single attractive impurity inside a 19-particle cluster made up of 18 ^{173}Yb atoms. The results are depicted in Fig. 4 and Fig. 5. In the first one, we can see the evolution of the total energy of the cluster, in units of $\hbar\omega$, as a function of the ^{173}Yb - ^{171}Yb interaction parameter, $g_{1D}(173, 171)$. This can be connected to the perpendicular confinement frequency via Fig. 1. As a reference, the experimental value of the perpendicular constraint frequency given in Ref. 4 is $\omega_{\perp} = 2\pi \times 25$ kHz, that corresponds to $g_{1D}(173, 171) = -13.5 \hbar\omega\sigma$. The ^{173}Yb atoms can all have all the same spin and SU(1) symmetry, or being distributed in N sets, with N in the range 2-6, and SU(N) symmetries.

We can see that in the limit $g_{1D}(\alpha, \beta) \rightarrow 0$, the energies of the different clusters converge to their corresponding non-interacting limits, given by $[N(N_p/N)^2 + 1] \hbar\omega/2$, with N the number of ^{173}Yb types of spins. For all SU(N) cases, those energies also increase with the interaction parameter, approaching the same value for strong confinements. This is probably due to the related increase in the repulsive ^{173}Yb - ^{173}Yb interaction, that blurs the difference between a strong repulsive interaction and that derived from the Pauli exclusion principle [22], making equivalent SU(N) and SU(1) systems with the same number of particles [17]. The density profiles given in Fig. 5 are the standard ones for systems with impurities: that minority component is located at the center of the cluster, with minor variations due to the particular arrangement considered. For instance, we can see that, for the same confinement frequency, the fewer the ^{173}Yb components, the wider their distribution. This is simply due to Pauli's repulsion, and has to do with the fact that a couple of particles with the same spin can not be at the same position, something not forbidden to two ^{173}Yb atoms belonging to different species. On the other hand, the influence of the perpendicular confinement in the arrangement of the majority component is very minor, as can be seen in the lower panel of Fig. 5.

With the help of Fig. 6, we can see that the influence of the internal structure on the density profiles of clusters including 12 ^{173}Yb atoms and 12 ^{171}Yb ones is larger. In the definition given above, those are *balanced* systems, something that can be seen in the fact that the distribution of one isotope perfectly match the one of the other. The density profile of an arrangement with 12 equal-spin ^{173}Yb and 12 equal-spin ^{171}Yb atoms (labeled 12+12 in Fig. 6) is the wider of all the ones considered. This is in consonance with what we saw in the previous figure: the application of Pauli's principle for both sets of 12 atoms forbids two atoms of the same isotope to share the same spot, spreading the atoms further. If we go to systems with the same number of ^{171}Yb atoms, but with six sets of two ^{173}Yb different spins ($2 \times 6 + 12$), the previous restriction is released, producing thinner clusters. This trend explains the evolution of the profiles when they in-

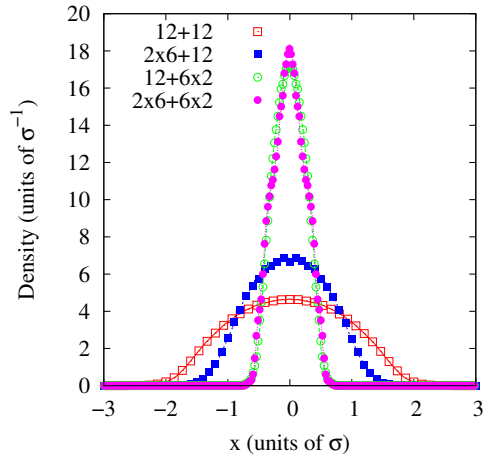


FIG. 6. Density profiles for a series of clusters including $N_p = 24$ particles, and for a ($\omega_{\perp} = 2\pi \times 25$ kHz). Symbols correspond to a profile that is the sum of all the 12 ^{173}Yb atoms, and lines to the 12 ^{171}Yb ones. The label $n_{173} \times m_{173} + n_{171} \times m_{171}$ means m_{173} sets of n_{173} ^{173}Yb with SU(m_{173}) symmetry and m_{171} sets of n_{171} ^{171}Yb spins with SU(m_{171}) symmetry.

clude two sets of 6 ^{171}Yb atoms: in this case, there are many pairs for which the Pauli's exclusion principle does not apply any more, allowing instead two ^{171}Yb atoms with different spins to weakly attract each other, concentrating in a smaller region. We can see also that the main driver of the collapsing of the density profile is the consideration of SU(2) symmetry in the ^{171}Yb atom set. The repulsive nature of the ^{173}Yb - ^{173}Yb interaction masks in part the effect of the Pauli exclusion avoidance.

On the other hand, the effect of varying the confinement in the profile of balanced clusters is, as in the impurity case, quite minor. In Fig. 7, we can see that, an increase in ω_{\perp} make the profiles slightly wider. The reason could be that, according to the results displayed in Fig. 1, the confinement increases the ^{173}Yb - ^{173}Yb repulsion, and this balances and slightly outweighs the corresponding increasing in the ^{173}Yb - ^{171}Yb attractive one.

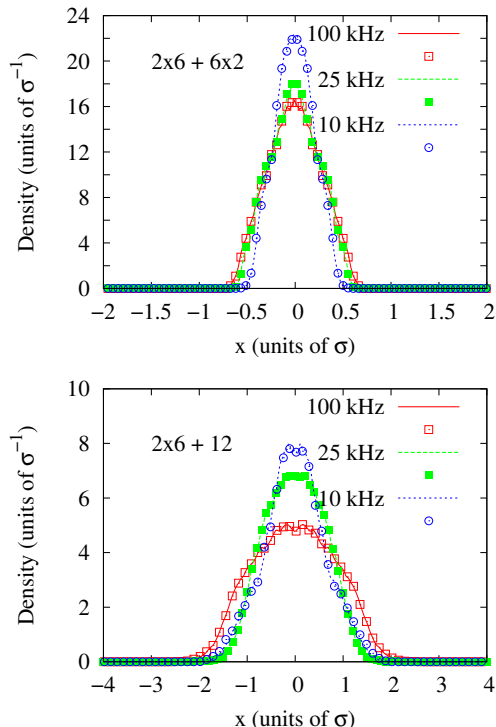


FIG. 7. Same as in the previous figure, but for different confinement frequencies.

IV. CONCLUSIONS

Summarizing, we can say that the main factor determining the structure of clusters of the same size and made up of different kind of fermions is Pauli's exclusion principle. The larger the number of different species, the smaller the number of atom pairs that cannot be on top of each other, and the thinner the clusters, with minor effects due to the magnitude of the perpendicular confinement. This effect increases appreciably when the interaction between spins belonging to different species is attractive instead of repulsive.

ACKNOWLEDGMENTS

We acknowledge financial support from MINECO (Spain) Grant FIS2017-84114-C2-2-P and Junta de Andalucía PAIDI group FQM-205. We also acknowledge the use of the C3UPO computer facilities at the Universidad Pablo de Olavide.

-
- [1] I. Bloch, J. Dalibard and W. Zwerger Rev. Mod. Phys. **80** 885 (2008).
- [2] M.A. Cazalilla and A.M. Rey. Rep. Prog. Phys. **77** 124401 (2014).
- [3] A. Goban, R. B. Hutson, G. E. Marti, S. L. Campbell, M. A. Perlin, P. S. Julienne, J. P. D'Incao, A. M. Rey, and J. Ye, Nature **563**, 369 (2018).
- [4] G. Pagano, M. Mancini, G. Cappellini, P. Lombardi, F. Schäfer, H. Hu, X.J. Liu, J. Catani, C. Sias, M. Inguscio and L. Fallani. Nat. Phys. **10** 198 (2014).
- [5] S. Taie, R. Yamazaki, S. Sugawa and Y. Takahashi. Nat. Phys. **8** 825 (2012).
- [6] H. Ozawa, S. Taie, Y. Takasu and Y. Takahashi. Phys. Rev. Lett. **121** 225303 (2018).
- [7] M. Kitagawa, K. Enomoto, K. Kasa, Y. Takahashi, R. Ciurylo, P. Naidon and P. S. Julienne, Phys. Rev. A **77** 012719 (2008).
- [8] S. Taie, Y. Takasu, S. Sugawa, R. Yamazaki, T. Tsujimoto, R. Murakami and Y. Takahashi. Phys. Rev. Lett. **105** 190401 (2010).
- [9] H. Hara, Y. Takasu, Y. Yamaoka, J. M. Doyle, and Y. Takahashi. Phys. Rev. Lett. **106** 205304 (2011).
- [10] S. Sugawa, K. Inaba, S. Taie, R. Yamakazi, M. Yamashita and Y. Takahashi. Nat. Phys. **7** 642 (2011).
- [11] S. Capponi, P. Lecheminat and K. Totsuka. Annals of Physics. **367** 50 (2016).
- [12] S. Xu, J. T. Barreiro, Y. Wang, and C. Wu. Phys. Rev. Lett. **121** 167205 (2018).
- [13] Y. Zhang, L. Vidmar, and M. Rigol. Phys. Rev. A **98** 042129 (2018).
- [14] Y. Zhang, L. Vidmar, and M. Rigol. Phys. Rev. A **99** 063605 (2019).
- [15] J. Decamp, J. Junemann, M. Albert, M. Rizzi, A. Minguzzi, and P. Vignolo, Phys. Rev. A **94**, 053614 (2016).
- [16] N. Matveeva and G. E. Astrakharchik, New J. Phys. **18**, 065009 (2016).
- [17] M.C. Gordillo, F. Mazzanti and J. Boronat. Phys. Rev. A **100** 023603 (2019).
- [18] M.C. Gordillo. New J. Phys. **21** 103020 (2019).
- [19] M. Olshanii. Phys. Rev. Lett. **81** 938 (1998).
- [20] B. L. Hammond, W.A. Lester, Jr., and P.J. Reynolds *Monte Carlo Methods in Ab Initio Quantum Chemistry* World Scientific. Singapore. (1994).
- [21] D.M. Ceperley. J. Stat. Phys. **63** 1237 (1991).
- [22] M.D. Girardeau. Phys. Rev. A **82** 011607(R) (2010).
- [23] M. Casula, D. M. Ceperley and E.J. Mueller. Phys. Rev. A **78** 033607 (2008).
- [24] G.E. Astrakharchik, *Quantum Monte Carlo Study Of Ultracold Gases*. PhD thesis, Università degli Studi di Trento (2004).
- [25] C. Carbonell-Coronado, F. De Soto and M.C. Gordillo. New. J. Phys. **18** 025015 (2016).
- [26] M.C. Gordillo and F. De Soto, Phys. Rev. A. **96** 013614 (2017).
- [27] M.C. Gordillo. Phys. Rev. A **96** 033630 1-5 (2017).

- [28] M.C. Gordillo. *J. Phys. B.* **51** 155301 1-6 (2018).
- [29] J. Carlson, S. Y. Chang, V. R. Pandharipande, and K. E. Schmidt, *Phys. Rev. Lett.* **91** 050401 (2003).
- [30] D.J. Griffiths, *Introduction to Quantum Mechanics* Benjamin Cummings. New Jersey (2004).
- [31] G.E. Astrakharchik, J. Boronat, J. Casulleras and S. Giorgini. *Phys. Rev. Lett.* **93** 200404 (2004).
- [32] R. J. Needs, M. D. Towler, N. D. Drummond, P. Lopez Rios, and J. R. Trail, *J. Chem. Phys.* **152** 154106 (2020).
- [33] M. Boninsegni, and S. Moroni, *Phys. Rev. E* **86** 056712 (2012).
- [34] J. Boronat and J. Casulleras, *Phys. Rev. B* **49**, 8920 (1994).